



General high-order solitons and breathers with a periodic wave background in the nonlocal Hirota–Maccari equation

Xiaolin Yang · Yi Zhang · Wenjing Li

Received: 25 October 2023 / Accepted: 22 December 2023 / Published online: 27 January 2024
© The Author(s), under exclusive licence to Springer Nature B.V. 2024

Abstract Soliton and breather solutions to the nonlocal Hirota–Maccari equation with a periodic wave background are constructed via the KP hierarchy reduction approach. By constraining tau functions of bilinear equations in the KP hierarchy, we obtain general $2N$ -line solitons and N -breather solutions with a periodic wave background. What needs to be emphasized are the two-soliton can be divided into non-degenerate and degenerate soliton according to the asymptotic analysis. Meanwhile, one- and two-breather solutions in a periodic wave and constant background are investigated.

Keywords Nonlocal Hirota–Maccari equation · Soliton solution · Breather solution · Periodic wave background · Kadomtsev–Petviashvili hierarchy reduction method

1 Introduction

The study of the dynamical behavior of physical systems has been, and continues to be, a major source of mathematical inspiration. In nonlinear physics, PT -symmetry can be used to describe energy transfer and wave behavior [1–5]. Due to the potential application in nonlinear optics, a new class of integrable

systems known as nonlocal models has just recently been proposed. The first PT -symmetric nonlocal integrable equation was introduced by Ablowitz and Muslimani [6]. In the past few years, some research on PT -symmetric equations has achieved new results in both theory and applications [7–12].

Nonlinear integrable equations can be solved in a variety of methods, such as the Darboux transformation [13], the Riemann–Hilbert approach [14], the Kadomtsev–Petviashvili (KP) hierarchy reduction method [15–17], and so on. Among them, the KP hierarchy reduction method is a powerful tool because it can bypass the spectral problem and the Lax pair of the equation and directly obtain the exact solution in a concise form.

In our recent work [18], inspired by Yang [19], a nonlocal Hirota–Maccari (HM) equation was proposed

$$\begin{aligned}u_t - iu_{xy} + \beta u_{xxx} + ur + \beta uu^*(-x, y, -t)u_x &= 0, \\ 3ir_x - (uu^*(-x, y, -t))_y &= 0,\end{aligned}\quad (1)$$

where u stands for the long wave, r is short wave and β is real parameter. By replacing $x \rightarrow ix$, $t \rightarrow -it$, $y \rightarrow -y$, the nonlocal HM equation reduces to the local Hirota–Maccari equation:

$$\begin{aligned}iu_t + u_{xy} + i\beta u_{xxx} + ur - i\beta |u|^2 u_x &= 0, \\ 3r_x + (|u|^2)_y &= 0,\end{aligned}\quad (2)$$

which comes from a higher-dimensional generalization of the Hirota equation [20–22]. Notably, compared to

X. Yang · Y. Zhang (✉) · W. Li
Department of Mathematics, Zhejiang Normal University,
Jinhua 321004, People's Republic of China
e-mail: zy2836@163.com

the local Eq. (2), this solution of the nonlocal Eq. (1) at position (x, t) relies on both the local solution at (x, t) and the nonlocal solution at $(-x, -t)$. Meanwhile, the nonlocal HM equation admits some interesting physical phenomenon for its new time- or space-coupling, which could lead to new physical consequences and encourage new practical applications [23]. From our work, we derived degenerate and non-degenerate solitons and examined the dynamical behavior of rational and lump-soliton solutions. Indeed, it is clearly richer than the variety of exact solutions in the local HM equation [24–26].

2 High-order solitons with a periodic background

General soliton solutions of Eq. (1) with a periodic wave background are examined in the part. To demonstrate the general $2N$ -soliton solutions of (1) on the periodic background, we first give the following Theorem. And the appendix includes relevant proofs.

Theorem 2.1 *The nonlocal (1) with a periodic wave background has soliton solutions*

$$u = \frac{g}{f}, \quad r = -2i(\ln f)_{xy}, \tag{3}$$

with f and g shown by determinants

$$f = \begin{pmatrix} c_i \delta_{ij} e^{-\chi_i} + \frac{1}{p_i + p_j^*} & \frac{1}{p_i - p_j^*} & \frac{1}{p_i - p_{2N+1}^*} \\ -\frac{1}{p_i - p_j^*} & -c_i^* \delta_{ij} e^{-\chi_i^*(-x, y, -t) - \frac{1}{p_i + p_j^*}} & -\frac{1}{p_i + p_{2N+1}^*} \\ \frac{1}{p_{2N+1} + p_j^*} & \frac{1}{p_{2N+1} - p_j^*} & i c_{2N+1} e^{-\chi_{2N+1}} + \frac{1}{p_{2N+1} - p_{2N+1}^*} \end{pmatrix}_{0 \leq i, j \leq N}, \tag{4}$$

$$g = \begin{pmatrix} c_i \delta_{ij} e^{-\chi_i} - \frac{p_i}{p_j^*} \frac{1}{p_i + p_j^*} & \frac{p_i}{p_j^*} \frac{1}{p_i - p_j^*} & \frac{p_i}{p_j^*} \frac{1}{p_i - p_{2N+1}^*} \\ -\frac{p_i}{p_j^*} \frac{1}{p_i - p_j^*} & -c_i^* \delta_{ij} e^{-\chi_i^*(-x, y, -t) + \frac{p_i}{p_j^*} \frac{1}{p_i + p_j^*}} & \frac{p_i}{p_{2N+1}^*} \frac{1}{p_i + p_{2N+1}^*} \\ -\frac{p_{2N+1}}{p_j^*} \frac{1}{p_{2N+1} + p_j^*} & \frac{p_{2N+1}}{p_j^*} \frac{1}{p_{2N+1} - p_j^*} & i c_{2N+1} e^{-\chi_{2N+1}} + \frac{p_{2N+1}}{p_{2N+1}^*} \frac{1}{p_{2N+1} - p_{2N+1}^*} \end{pmatrix}_{0 \leq i, j \leq N},$$

Furthermore, regarding soliton solutions studied on a periodic wave background also attracts attention. Tian and his group have discussed N -soliton solutions on the nonzero background in the Korteweg–de Vries–Calogero–Bogoyavlenskii–Schif equation [27]. Rao and his collaborators have studied various kinds of solutions on a periodic background to the Dave–Stewartson I equation [28]. Zha et al. have investigated breathers and rogue waves on a double-periodic wave background in the Gerdjikov–Ivanov equation [29]. It should be noted that the local HM equation don't have the soliton solutions with a periodic wave background. Thus, a natural motivation is to use the KP hierarchy reduction method to study the dynamical behavior of a periodic wave background in the nonlocal HM equation.

The structure is as follows. The characteristics of line solitons in Eq. (1) are described and examined in Sect. 2. In Sect. 3, we are committed to investigating the breather solutions on both a constant and periodic background. In Sect. 4, we discuss the solutions in detail. Section 5 is the conclusion.

and

$$\chi_i = \frac{2p_i R x}{\sqrt{6}} - 2p_i R p_{iI} y - \frac{\sqrt{6}}{9}(\beta t + x)(2p_{iR}^3 - 6p_{iR} p_{iI}^2) + \chi_{0,i},$$

$$\chi_{2N+1} = \frac{2ip_{2N+1, I} x}{\sqrt{6}} - 2p_{2N+1, R} p_{2N+1, I} y - \frac{\sqrt{6}}{9}(\beta t + x)(6ip_{2N+1, R}^2 p_{2N+1, I} - 2ip_{2N+1, I}^3) + \chi_{0,2N+1}, \tag{5}$$

where δ_{ij} is the Kronecker symbol, c_i, p_i are complex, $\chi_{0,i}$ are real for $i = 0, 1, \dots, N$, and p_{2N+1} is imaginary number.

To better understand the actions of the line solitons with a periodic wave background, we take $N = 0$ in Theorem (2.1), then f, g could be denoted as

$$f = ic_1 e^{l-\chi_{0,1}} + \frac{1}{2ip_{1I}},$$

$$g = ic_1 e^{l-\chi_{0,1}} + \frac{1}{2ip_{1I}} \frac{p_{1R} + ip_{1I}}{p_{1R} - ip_{1I}}, \tag{6}$$

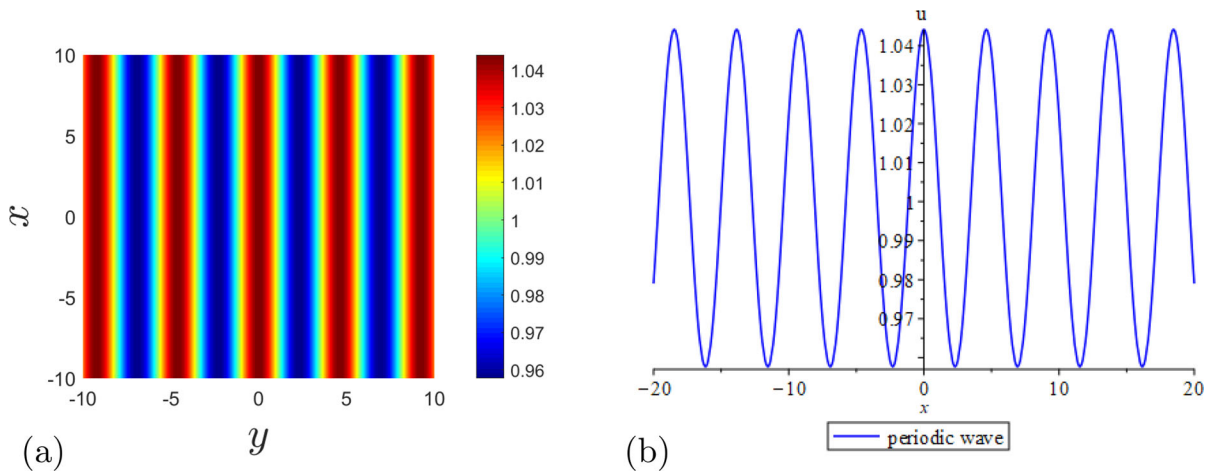


Fig. 1 Periodic wave solution with $\beta = 2, b_1 = \frac{1}{4}, p_1 = i, \chi_{0,1} = \pi$

where $l = -\frac{2p_{1R}x}{\sqrt{6}} + 2p_{1R}p_{1I}y + \frac{\sqrt{6}}{9}(\beta t + x)(2p_{1R}^3 - 6p_{1R}p_{1I}^2)$.

As discussed in Ref. [30], in order to avoid the solution being singular, we take $p_{1R} = 0$. Then the solution is independent of y . It is important to emphasize that $\chi_{0,1}$ controls the amplitude of periodic wave. Fig. 1 shows the periodic wave.

Further, the two-soliton solution with a periodic wave background is derived when setting $N = 1$ and the expressions for f_1, g_1 are given

$$\begin{aligned}
 f_1 &= \begin{pmatrix} c_1 e^{-\chi_1} + \frac{1}{p_1 + p_1^*} & \frac{1}{p_1 - p_1^*} & \frac{1}{p_1 - p_3^*} \\ -\frac{1}{p_1 - p_1^*} & -c_1^* e^{-\chi_1^*(-x, y, -t) - \frac{1}{p_1 + p_1^*}} & -\frac{1}{p_1 + p_3^*} \\ \frac{1}{p_3 + p_1^*} & \frac{1}{p_3 - p_1^*} & ic_3 e^{-\chi_3} + \frac{1}{p_3 - p_3^*} \end{pmatrix}, \\
 g_1 &= \begin{pmatrix} c_1 e^{-\chi_1} - \frac{p_1}{p_1^*} \frac{1}{p_1 + p_1^*} & \frac{p_1}{p_1^*} \frac{1}{p_1 - p_1^*} & \frac{p_1}{p_3^*} \frac{1}{p_1 - p_3^*} \\ -\frac{p_1}{p_1^*} \frac{1}{p_1 - p_1^*} & -c_1^* e^{-\chi_1^*(-x, y, -t) + \frac{p_1}{p_1^*} \frac{1}{p_1 + p_1^*}} & \frac{p_1}{p_3^*} \frac{1}{p_1 + p_3^*} \\ -\frac{p_3}{p_1^*} \frac{1}{p_3 + p_1^*} & \frac{p_3}{p_1^*} \frac{1}{p_3 - p_1^*} & ic_3 e^{-\chi_3} + \frac{p_3}{p_3^*} \frac{1}{p_3 - p_3^*} \end{pmatrix},
 \end{aligned} \tag{7}$$

where f_1, g_1 both are 3×3 determinants and

$$\begin{aligned}
 \chi_1 &= \frac{2p_{1R}x}{\sqrt{6}} - 2p_{1R}p_{1I}y - \frac{\sqrt{6}}{9}(\beta t + x)(2p_{1R}^3 - 6p_{1R}p_{1I}^2) + \chi_{0,1}, \\
 \chi_3 &= \frac{2ip_{3I}x}{\sqrt{6}} - 2p_{3R}p_{3I}y - \frac{\sqrt{6}}{9}(\beta t + x)(6ip_{3R}^2 p_{3I} - 2ip_{3I}^3) + \chi_{0,3}.
 \end{aligned} \tag{8}$$

The patterns of the two-soliton solution with a periodic wave background are the same as those with a constant background due to the soliton interacts elastically with the periodic line waves.

In what follows, by removing the third row and third column of the determinant (7), we explore the asymptotic results for two soliton. The asymptotic soliton along the two lines $\frac{2p_{1R}x}{\sqrt{6}} - 2p_{1R}p_{1I}y - \frac{\sqrt{6}}{9}(\beta t + x)(2p_{1R}^3 - 6p_{1R}p_{1I}^2) + \chi_{0,1}$ and $-\frac{2p_{1R}x}{\sqrt{6}} - 2p_{1R}p_{1I}y +$

$\frac{\sqrt{6}}{9}(\beta t + x)(2p_{1R}^3 - 6p_{1R}p_{1I}^2) + \chi_{0,1}$, which have some different results:

- (i) Before collision ($x \rightarrow -\infty$)
Soliton 1 ($\chi_1 \approx 0, \chi_1^*(-x, y, -t) \rightarrow +\infty$):

$$u_1^- \simeq \frac{c_1 e^{-\chi_1} - \frac{1}{p_1 + p_1^*} \frac{p_1}{p_1^*}}{c_1 e^{-\chi_1} + \frac{1}{p_1 + p_1^*}}, \tag{9}$$

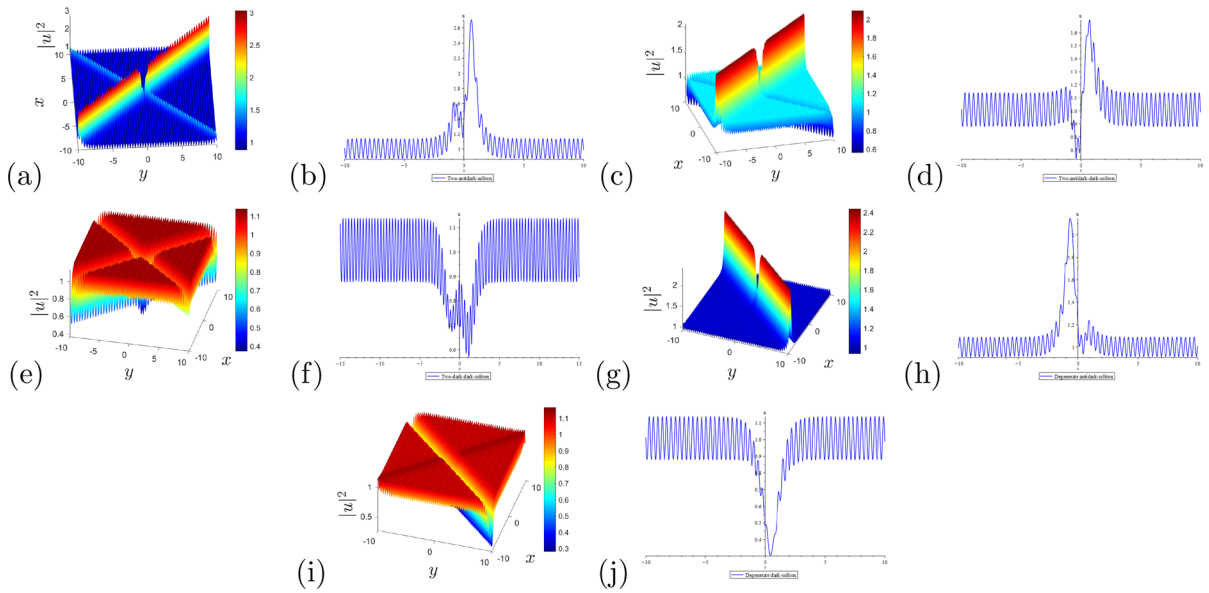


Fig. 2 Five types of the two line-soliton solutions at $t = 5$ with $p_1 = -1 - i, p_3 = -3i, c_3 = \frac{i}{4}, \chi_{0,1} = 0, \chi_{0,3} = \pi$. **a, b** Two antidark-soliton solution with $c_1 = 1 + i$. **c, d** A antidark-dark-soliton solution with $c_1 = 1 + \frac{i}{2}$. **e, f** Two dark-soliton

solution with $c_1 = -1 - 2i$. **g, h** Degenerate dark-soliton solution with $c_1 = 1 - i$. **i, j** Degenerate antidark-soliton solution with $c_1 = 1 + i$

Soliton 2 ($\chi_1^*(-x, y, -t) \approx 0, \chi_1 \rightarrow -\infty$):

$$u_2^- \simeq -\frac{p_1 c_1^* e^{-\chi_1^*(-x,y,-t)+\theta} - \frac{1}{p_1+p_1^*} \frac{p_1}{p_1^*}}{p_1^* c_1^* e^{-\chi_1^*(-x,y,-t)+\theta} + \frac{1}{p_1+p_1^*}}, \tag{10}$$

where $e^\theta = -\frac{(p_1-p_1^*)^2}{4p_1 p_1^*}$.

(ii) After collision ($x \rightarrow +\infty$)

Soliton 1 ($\chi_1 \approx 0, \chi_1^*(-x, y, -t) \rightarrow -\infty$):

$$u_1^+ \simeq -\frac{p_1 c_1 e^{-\chi_1+\theta} - \frac{1}{p_1+p_1^*} \frac{p_1}{p_1^*}}{p_1^* c_1 e^{-\chi_1+\theta} + \frac{1}{p_1+p_1^*}}, \tag{11}$$

Soliton 2 ($\chi_1^*(-x, y, -t) \approx 0, \chi_1 \rightarrow +\infty$):

$$u_2^+ \simeq \frac{c_1^* e^{-\chi_1^*(-x,y,-t)} - \frac{1}{p_1+p_1^*} \frac{p_1}{p_1^*}}{c_1^* e^{-\chi_1^*(-x,y,-t)} + \frac{1}{p_1+p_1^*}}, \tag{12}$$

Since $u_1^+(\chi_1) = (-\frac{p_1}{p_1^*})u_1^-(\chi_1 - \theta)$ and $|\frac{p_1}{p_1^*}| = 1$, thus these properties imply that the amplitude and velocity of the two-soliton are the same before and after collision. Meanwhile, $|u_j|$ has a maximum value expressed as $|u_j|_{max}$ along the line $\chi_j - \frac{1}{2} \ln(4p_{1,R}^2(c_{1,R}^2 + c_{1,I}^2)) = 0$ for $j = 1, 2$. According to the above analysis, Fig. 2 displays all forms of the two-soliton, namely, two-antidark-antidark-soliton

(see Fig. 2a, b), two-dark-antidark-soliton (see Fig. 2c, d), two-dark-dark-soliton (see Fig. 2e, f), degenerate two-antidark soliton (see Fig. 2g, h), degenerate two-dark soliton (see Fig. 2i, j).

We could also gain the higher-order line solitons with a periodic wave background. When $N = 2$, there are several patterns of the non-degenerate four-soliton solutions, and three of them are shown in the Fig. 3.

3 Breathers with a constant and periodic background

Breather solutions are studied from two distinct backgrounds, namely the constant background and the periodic wave background in this part. We express these solutions in terms of determinants in the following theorem.

Theorem 3.1 *The nonlocal HM Eq. (1) has breather solutions*

$$u = \frac{g}{f}, \quad r = -2i(\ln f)_{xy}, \tag{13}$$

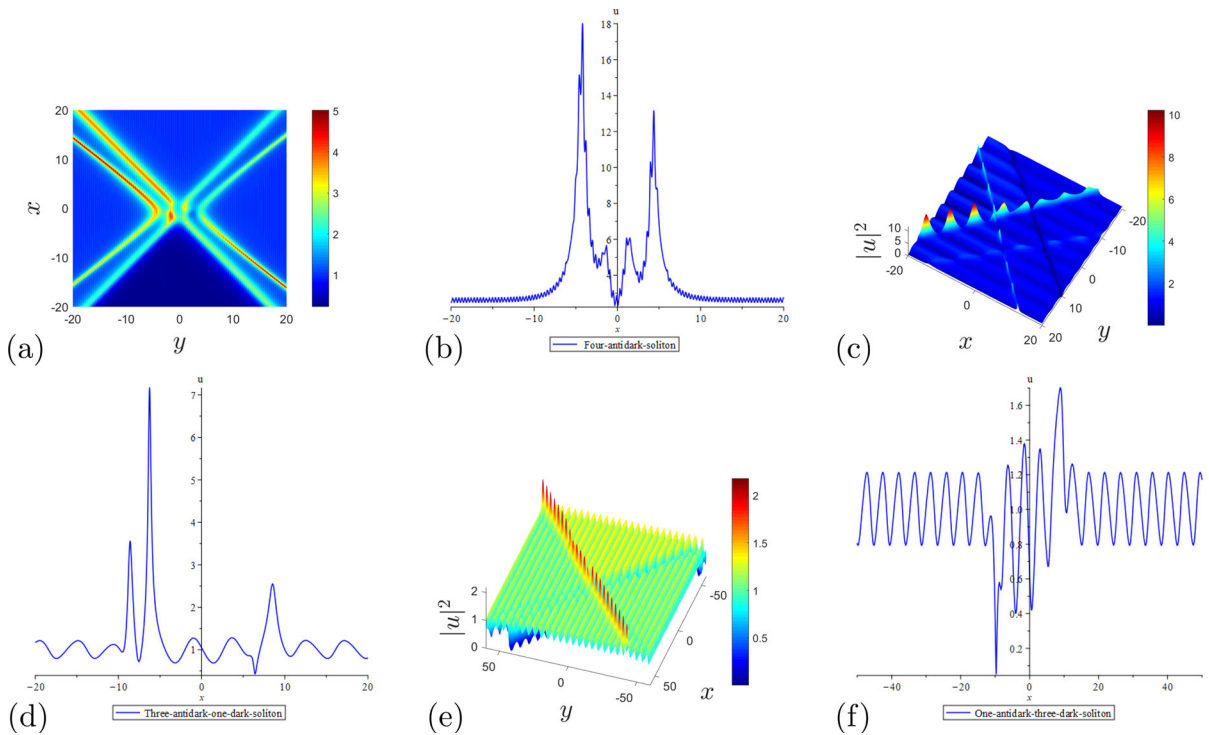


Fig. 3 The four-soliton solution at $t = 0$. **a, b** Non-degenerate four-antidark-soliton solution with $p_1 = -\frac{1}{2} - \frac{i}{2}, p_2 = -1 - \frac{4i}{5}, p_5 = -3i, c_1 = 1 + \frac{i}{2}, c_2 = 1 + \frac{2i}{5}, c_5 = -\frac{i}{4}, \chi_{0,1} = 0, \chi_{0,2} = 0, \chi_{0,5} = -\pi$. **c, d** Non-degenerate three-antidark-one-dark-soliton solution with $p_1 = -\frac{1}{2} - i, p_2 = -1 - i, p_5 =$

$-i, c_1 = 1 + 2i, c_2 = 1 + \frac{i}{2}, c_5 = -i, \chi_{0,1} = 3\pi, \chi_{0,2} = -3\pi, \chi_{0,5} = -\frac{\pi}{2}$. **e, f** Non-degenerate one-antidark-three-dark-soliton solution with $p_1 = -\frac{1}{2} - i, p_2 = 1 - i, p_5 = -i, c_1 = 1 + 2i, c_2 = 1 + \frac{i}{2}, c_5 = -i, \chi_{0,1} = 3\pi, \chi_{0,2} = -3\pi, \chi_{0,5} = -\frac{\pi}{2}$

with f and g are:

$$f = \Lambda \left| \frac{\delta_{ij}}{\omega_i e^{\lambda_i x}} + \frac{1}{\frac{1}{2}(\omega_i + \omega_j) + i(\lambda_i - \lambda_j)} \right|_{1 \leq i, j \leq N},$$

$$g = \Lambda \left| \frac{\delta_{ij}}{\omega_i e^{\lambda_i x}} - \frac{\omega_i + 2i\lambda_i}{\omega_j - 2i\lambda_j} \frac{1}{\frac{1}{2}(\omega_i + \omega_j) + i(\lambda_i - \lambda_j)} \right|_{1 \leq i, j \leq N},$$

(14)

and

$$\zeta_i = \frac{1}{\sqrt{6}} i \omega_i x + \beta \omega_i \lambda_i y - \frac{\sqrt{6}}{9} i \left(\frac{\omega_i^3}{4} - 3\omega_i \lambda_i^2 \right) (\beta t + x) + \chi_{0,i},$$

(15)

where $\Lambda = \prod_{i=1}^N \omega_i e^{\lambda_i x}$, and $\omega_i, \lambda_i, \chi_{0,i}$ are real-valued parameters.

Remark 3.1 Depending on the parameter constraints, periodic waves have two dynamical behaviors:

- When $N = 2K, \omega_{K+j} = -\omega_j, \lambda_{K+j} = -\lambda_j, \chi_{0,K+i} = \chi_{0,i}$, the breather with a constant background can be obtained.
- When $N = 2K + 1, \omega_{K+j} = -\omega_j, \lambda_{K+j} = -\lambda_j, \chi_{0,K+i} = \chi_{0,i}, \lambda_{2K+1} = 0$, we yield the breather with a periodic wave background.

In what follows, we construct the breather in the constant background. To this end, by choosing

$$N = 2, \quad \omega_2 = -\omega_1, \quad \lambda_2 = -\lambda_1, \quad \zeta_{0,2} = \zeta_{0,1},$$

(16)

and the resulting breather read

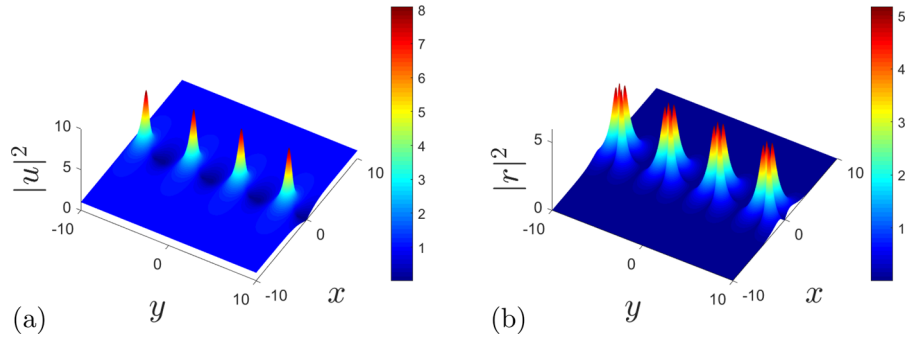
$$u = \frac{g}{f}, \quad r = -2i(\ln f)_{xy},$$

(17)

with

$$f = \left| \begin{array}{cc} \frac{1}{\omega_1 e^{\lambda_1 x}} + \frac{1}{\omega_1} & \frac{1}{2i\lambda_1} \\ \frac{1}{-2i\lambda_1} & \frac{1}{-\omega_1 e^{\lambda_1 x}} - \frac{1}{\omega_1} \end{array} \right|,$$

Fig. 4 One-breather at $t = 0$ with $\lambda_1 = 2, \omega_1 = 2, \beta = 1, \zeta_{0,1} = 0$



$$g = \left| \begin{array}{cc} \frac{1}{\omega_1 e^{\zeta_1}} - \frac{\omega_1 + 2i\lambda_1}{\omega_1 - 2i\lambda_1} \frac{1}{\omega_1} & \frac{\omega_1 + 2i\lambda_1}{\omega_1 - 2i\lambda_1} \frac{1}{2i\lambda_1} \\ -\frac{\omega_1 + 2i\lambda_1}{\omega_1 - 2i\lambda_1} \frac{1}{2i\lambda_1} & -\frac{1}{\omega_1 e^{\zeta_1^*}} + \frac{\omega_1 + 2i\lambda_1}{\omega_1 - 2i\lambda_1} \frac{1}{\omega_1} \end{array} \right|.$$

After a simple algebraic calculation, the final form of the breather solution reads

$$u = \frac{(-16\lambda_1^4 + 16i\lambda_1^3\omega_1 + 4i\lambda_1\omega_1^3 + \omega_1^4)e^{2c_1R} + 16\left(-\frac{\omega_1^2}{4} - \lambda_1^3\right)e^{c_1^*} + \left(\frac{\omega_1^2}{4} + \lambda_1^2\right)e^{c_1} + i\omega_1\lambda_1 - \frac{\omega_1^2}{4} + \lambda_1^2\lambda_1^2}{(4(i\lambda_1 - \frac{\omega_1}{2})^2((4\lambda_1^2 + \omega_1^2)e^{2c_1R} + 4\lambda_1^2(e^{c_1} + e^{c_1^*} + 1))),} \cdot \left(-\left(\frac{1}{\omega_1^2} + \frac{1}{4\lambda_1^2} + \frac{1}{\omega_1^2 e^{c_1}} + \frac{1}{\omega_1^2 e^{c_1^*}} + \frac{1}{\omega_1^2 e^{2c_1R}}\right)\right)_{xy}. \tag{18}$$

The above solution contains trigonometric functions, thus the solution is periodic as $c_1 = c_{1R} + ic_{1I}$. Notably, the periodic solution does not progress in the y direction. Fig. 4 illustrates one breather for two independent variables.

With a larger K , the N -breathers with the constant background could be given. In this case, we take $K = 2$, the corresponding solution has two individual breathers, and possesses interesting involution patterns. In order to observe the more interesting phenomenon of the two breathers, we fix the value of $\chi_{0,1}$ and take different values of $\chi_{0,2}$. Hence, we take the following parameters choices:

$$\begin{aligned} \lambda_1 = 2, \quad \lambda_2 = 2, \quad \lambda_3 = -2, \quad \lambda_4 = -2, \\ \omega_1 = 2, \quad \omega_2 = \frac{1}{2}, \\ \omega_3 = -2, \quad \omega_4 = -\frac{1}{2}, \quad \beta = 1, \quad \chi_{0,1} = 0. \end{aligned} \tag{19}$$

With the parameter choices described above, Fig. 5 shows the evolutionary patterns of the two breathers. One can directly find that $\chi_{0,1}$ controls breather-1 and $\chi_{0,2}$ controls breather-2. When $\chi_{0,2} \ll 0$, there is a large distance between the two breathers. When

$\chi_{0,2} \rightarrow 0$, two breathers are in close proximity and start interacting. When $\chi_{0,2} \gg 0$, two breathers will first form a single breather, after which the two breathers will separate from each other. We find the collision between two breathers is an elastic collision.

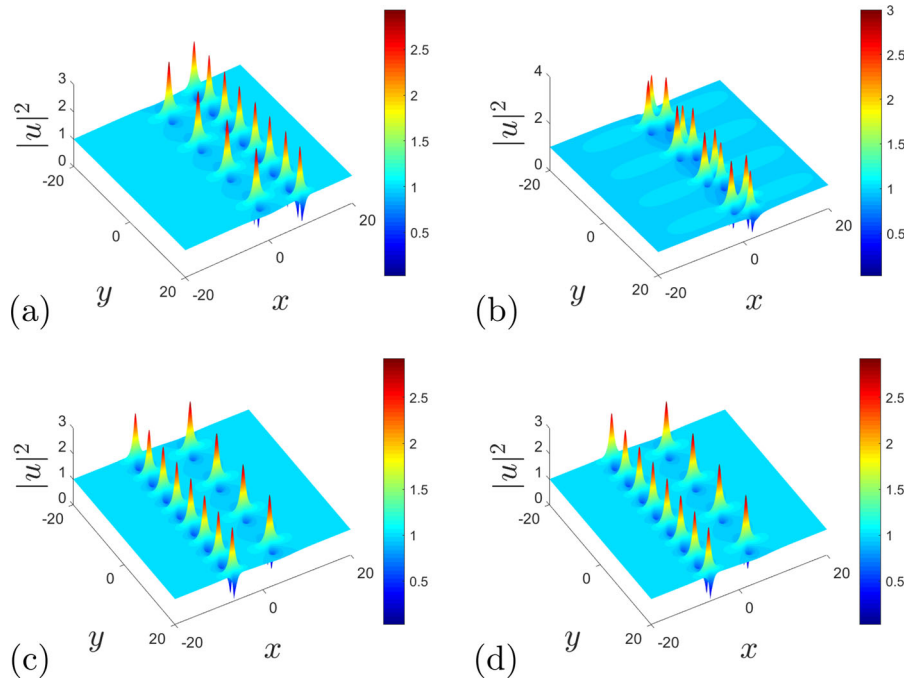
In order to examine the moving features of breathers with a periodic wave background, by taking $K = 1$ and the parameters are satisfying

$$\begin{aligned} \omega_2 = -\omega_1, \quad \lambda_2 = -\lambda_1, \\ \lambda_3 = 0, \quad \chi_{0,2} = \chi_{0,1}, \end{aligned} \tag{20}$$

then we obtain one breather with a periodic wave background

$$u = \frac{g_2}{f_2}, \tag{21}$$

Fig. 5 The two-breather solution on a constant background with parameters: **a** $\chi_{0,2} = -2\pi$; **b** $\chi_{0,2} = -\frac{\pi}{2}$; **c** $\chi_{0,2} = 0$; **d** $\chi_{0,2} = 2\pi$



where f and g are

$$f_2 = \begin{pmatrix} \frac{1}{\omega_1 e^{\lambda_1}} + \frac{1}{\omega_1} & \frac{1}{2i\lambda_1} & \frac{1}{\frac{1}{2}(\omega_1 + \omega_3) + i\lambda_1} \\ \frac{1}{-2i\lambda_1} & \frac{1}{-\omega_1 e^{\lambda_1^*}} - \frac{1}{\omega_1} & \frac{1}{\frac{1}{2}(\omega_2 + \omega_3) + i\lambda_2} \\ \frac{1}{\frac{1}{2}(\omega_3 + \omega_1) - i\lambda_1} & \frac{1}{\frac{1}{2}(\omega_3 + \omega_2) - i\lambda_2} & \frac{1}{\omega_3 e^{\lambda_3}} + \frac{1}{\omega_3} \end{pmatrix},$$

$$g_2 = \begin{pmatrix} \frac{1}{\omega_1 e^{\lambda_1}} - \frac{\omega_1 + 2i\lambda_1}{\omega_1 - 2i\lambda_1} \frac{1}{\omega_1} & \frac{\omega_1 + 2i\lambda_1}{\omega_1 - 2i\lambda_1} \frac{1}{2i\lambda_1} & -\frac{\omega_1 + 2i\lambda_1}{\omega_3} \frac{1}{\frac{1}{2}(\omega_1 + \omega_3) + i\lambda_1} \\ -\frac{\omega_1 + 2i\lambda_1}{\omega_1 - 2i\lambda_1} \frac{1}{-2i\lambda_1} & \frac{1}{-\omega_1 e^{\lambda_1^*}} + \frac{\omega_1 + 2i\lambda_1}{\omega_1 - 2i\lambda_1} \frac{1}{\omega_1} & -\frac{\omega_2 + 2i\lambda_2}{\omega_3} \frac{1}{\frac{1}{2}(\omega_2 + \omega_3) + i\lambda_2} \\ -\frac{\omega_3}{\omega_1 - 2i\lambda_1} \frac{1}{\frac{1}{2}(\omega_3 + \omega_1) - i\lambda_1} & -\frac{\omega_3}{\omega_2 - 2i\lambda_2} \frac{1}{\frac{1}{2}(\omega_3 + \omega_2) - i\lambda_2} & \frac{1}{\omega_3 e^{\lambda_3}} - \frac{1}{\omega_3} \end{pmatrix},$$
(22)

and

$$\chi_1 = \frac{1}{\sqrt{6}} i \omega_1 x + \lambda_1 \omega_1 y - \frac{\sqrt{6}i}{9}$$

$$\left(\frac{\omega_1^3}{4} - 3\lambda_1^2 \omega_1 \right) (x + t) + \chi_{0,1},$$

$$\chi_3 = \frac{i}{\sqrt{6}} \omega_3 x - \frac{\sqrt{6}i}{9} \frac{\omega_1^3}{4} (t + x) + \chi_{0,3}. \tag{23}$$

Based on the analysis of the solution, we thus conclude that the breather remains periodic in the (x, t) plane and localizes along y . The location of one breather is determined by $\chi_{0,3}$. Figure 6 illustrates different dynamics of the one-breather with distinct $\chi_{0,3}$.

Similarly, high order breathers with a periodic wave background are obtained from the Theorem (3.1). For example, we take $K = 2$ and

$$\lambda_5 = 0, \quad \lambda_3 = -\lambda_1, \quad \lambda_4 = -\lambda_2,$$

$$\omega_3 = -\omega_1, \quad \omega_4 = -\omega_2 \tag{24}$$

the two breathers with a periodic wave background would be derived. According to the different values of $\chi_{0,1}$, the two breathers will be displayed in Fig. 7.

4 Discussion on solutions

In this section, we mainly discuss the influence of parameters on the solutions. By substituting two inde-

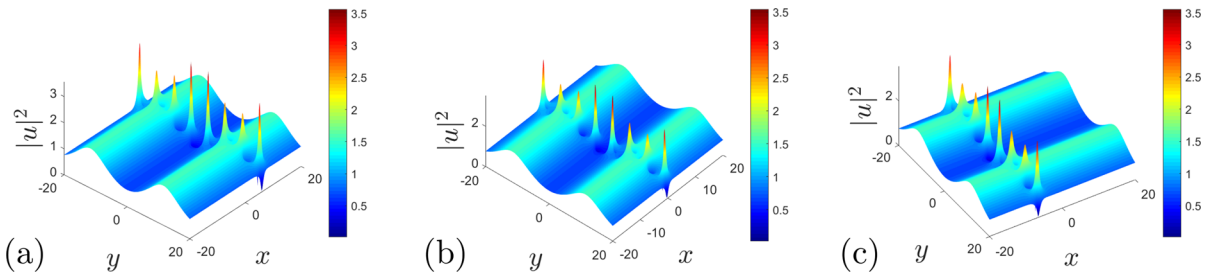


Fig. 6 One-breather with a periodic wave background at $t = 1$ with: **a** $\chi_{0,2} = -2\pi$; **b** $\chi_{0,2} = 0$; **c** $\chi_{0,2} = 2\pi$

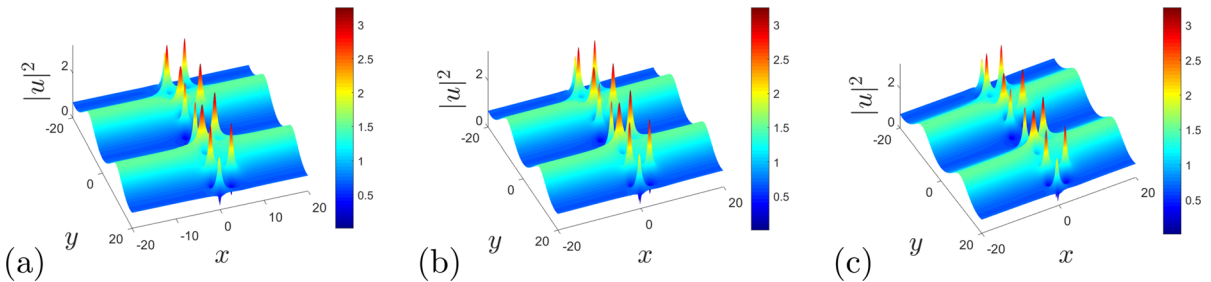


Fig. 7 Two-breather solution with a periodic wave background at $t = 1$ with $\lambda_1 = 2, \lambda_2 = 2, \omega_1 = 1, \omega_2 = \frac{1}{2}, \omega_5 = 1, \chi_{0,3} = 0, \chi_{0,5} = \frac{4\pi}{5}$: **a** $\chi_{0,1} = -10\pi$; **b** $\chi_{0,1} = -\frac{\pi}{2}$; **c** $\chi_{0,1} = 10\pi$

pendent variables in the τ function, soliton solutions and breather solutions can be constructed respectively. For line solitons on the periodic wave background, when $N = 0$, the periodic wave is shown in Fig. 1. If $N = 1$, through asymptotic analysis, we conclude that $u_1^+(\chi_1) = (-\frac{p_1}{p_1^*})u_1^-(\chi_1 - \theta)$ and $|\frac{p_1}{p_1^*}| = 1$. The elastic collision of two-soliton occurs at this time, including degenerate soliton and non-degenerate soliton. With respect to general two-soliton, $|u|$ component possesses five dynamical patterns with a periodic wave background (see Fig. 2), while $|r|$ component only appears the two-antidark-antidark-soliton. Meanwhile, the high-order line soliton solutions with a periodic wave background are demonstrated (see Fig. 3).

In the case of introducing parameters $p_i = \frac{\omega_i}{2} + i\lambda_i, q_i = \frac{\omega_i}{2} - i\lambda_i$, we derive the breather solutions. To manipulate the breathers in both constant and periodic wave background, our careful adjustment involves dividing the determinant's order in Eq. (41). When $N = 2K, \omega_{K+j} = -\omega_j, \lambda_{K+j} = -\lambda_j, \chi_{0,K+i} = \chi_{0,i}$, the breather with a constant background can be obtained, as shown in Fig. 4-5. When we fix $\chi_{0,1}$ and take different values for $\chi_{0,2}$, the two breathers will interact. It's fascinating that two breathers will exhibit a triangular pattern in the case of $\chi_{0,2}$ is close to $\chi_{0,1}$. Conversely, if

$N = 2K + 1, \omega_{K+j} = -\omega_j, \lambda_{K+j} = -\lambda_j, \chi_{0,K+i} = \chi_{0,i}, \lambda_{2K+1} = 0$, we acquire the breathers within the periodic wave background (see Fig. 6-7). As for the rational solutions obtained by taking the long wave limit on the periodic solutions, we have studied it in Ref. [18].

5 Conclusion

In this paper, we mainly utilize the KP reduction method to construct the solitons and breathers with a periodic wave background in Eq. (1). Taking different parameter constraints on the tau functions, the $2N$ solitons and the N breather solutions with a periodic wave background could be expressed. Within the background of a periodic wave, line solitons exhibit a classification of five distinct wave types. The breathers on both the constant background and the periodic wave background can be formed when the order of the determinant (41) is either odd or even. Elastic collisions between two breathers are observed through an analysis of their dynamic behavior on a constant background. It is apparent that when the order of the determinant increases, the period of the periodic wave also strengthens. Besides, the form of these solutions that we obtain

is more concise and meaningful for the research of non-linear mathematical physical models.

Acknowledgements This work was supported by the National Natural Science Foundation of China (Grant Nos. 11371326, 11975145 and 12271488).

Data Availability Statement All data generated or analyzed during this study are included in this published article.

Declarations

Conflict of interest The authors declare that there is no conflict of interests regarding the research effort and the publication of this paper.

Appendix A

In this part, we will prove the Theorem (2.1) and Theorem (3.1). Firstly, we utilize the variable transformations

$$u = \frac{g}{f}, \quad u^*(-x, y, -t) = \frac{h}{f}, \quad r = -2i(\ln f)_{xy}, \tag{25}$$

to convert the Eq. (2) into the bilinear equation

$$\begin{aligned} (D_t - iD_x D_y + \beta D_x^3 + \beta D_x)g \cdot f &= 0, \\ (3D_x^2 + 1)f \cdot f &= gh. \end{aligned} \tag{26}$$

Taking reduction condition

$$(\partial_x - \partial_s)f = cf, \tag{27}$$

the (3 + 1) dimensional system of Eq. (1) can be obtained

$$\begin{aligned} (D_t - iD_x D_y + \beta D_x^3 + \beta D_x)g \cdot f &= 0, \\ (3D_x D_s + 1)f \cdot f &= gh, \end{aligned} \tag{28}$$

under the nonlocal condition

$$f(x, y, t)g^*(-x, y, -t) = f^*(-x, y, -t)h(x, y, t), \tag{29}$$

where c is constant, g, h are complex-valued functions, and f is a real-valued function.

Based on the Sato theory [31,32], the bilinear equations in the KP hierarchy

$$\begin{aligned} (D_{x_1}^3 + 3D_{x_1} D_{x_2} - 4D_{x_3})\tau_{n+1}\tau_n &= 0, \\ (D_{x_1} D_{x_{-1}} - 2)\tau_n \tau_n &= -2\tau_{n+1}\tau_{n-1}, \end{aligned} \tag{30}$$

exist the determinant

$$\tau_n = \frac{\det (m_{ij}^{(n)})}{1 \leq i, j \leq N}, \tag{31}$$

where

$$\begin{aligned} m_{ij}^{(n)} &= \tilde{c}_i \delta_{ij} + \frac{p_i + s_i}{p_i + q_j} \left(\frac{-p_i}{q_j} \right)^n e^{\xi_i + \eta_j}, \\ \xi_i &= \frac{1}{p_i} x_{-1} + p_i x_1 + p_i^2 x_2 + p_i^3 x_3 + \xi_{0,i}, \\ \eta_j &= \frac{1}{q_j} x_{-1} + q_j x_1 - q_j^2 x_2 + q_j^3 x_3 + \eta_{0,j}. \end{aligned} \tag{32}$$

In order to obtain periodic solutions, we employ the independent variables $x_1 = \frac{1}{\sqrt{6}}x, x_2 = \frac{1}{2}i\beta y, x_3 = -\frac{\sqrt{6}}{9}\beta t - \frac{\sqrt{6}}{9}x$, then the Eq. (31) can rewrite

$$\tau_n = \prod_{i=1}^N (p_i + s_i) e^{\xi_i} \widehat{\det (m_{ij}^{(n)})}, \tag{33}$$

where

$$\widehat{m_{ij}^{(n)}} = \tilde{c}_i \delta_{ij} e^{-\zeta_i} \frac{1}{p_i + s_i} + \frac{1}{p_i + q_j} \left(\frac{-p_i}{q_j} \right)^n, \tag{34}$$

with

$$\begin{aligned} \zeta_i &= \xi_i + \eta_i \\ &= \frac{1}{\sqrt{6}}(p_i + q_j)x + \frac{i}{2}\beta(p_i^2 - q_j^2)y \\ &\quad - \frac{\sqrt{6}}{9}(\beta t + x)(p_i^3 + q_j^3) + \chi_{0,i}. \end{aligned} \tag{35}$$

To yield soliton solutions, we consider $M = 2N + 1$ in Eq. (31) and restrict the parameters obeying the following conditions

$$\begin{aligned} s_j &= -p_j + 1, \quad p_{M+i} = -p_i, \quad q_{M+i} = -q_i, \quad q_i = p_i^*, \\ q_{2M+1} &= -p_{2M+1}^*, \quad \tilde{c}_j = b_j, \quad c_{M+i} = -c_i^*, \quad \widehat{c_{2M+1}} = ic_{2M+1}, \end{aligned} \tag{36}$$

then one can obtain

$$\begin{aligned} \chi_{2M+1}^*(-x, y, -t) &= \chi_{2M+1}(x, y, t), \\ \chi_{M+i}^*(-x, y, -t) &= \chi_i(x, y, t), \end{aligned} \tag{37}$$

and derive

$$\begin{aligned} \widehat{m_{M+i,j}^{*(n)}}(-x, y, -t) &= -c_i^* \delta_{M+i,j} e^{-\chi_i} \\ &\quad - \frac{1}{p_i^* + p_{M+j}} \left(\frac{-p_{M+j}}{p_i^*} \right)^{-n} \\ &= -\widehat{m_{i,M+j}^{(n)}}(-x, y, t), \end{aligned} \tag{38}$$

which implies

$$\tau_n^*(-x, y, -t) = (-1)^{3N} \tau_{-n}(x, y, t). \tag{39}$$

As a result, Eq. (30) can be reduced to the bilinear Eqs.(28) with $f = \tau_0, g = \tau_1, h = \tau_{-1}$.

To generate breathers to Eq. (1), we select several variable transformations

$$\begin{aligned} x_{-1} &= -\frac{1}{\sqrt{6}}is, & x_1 &= \frac{1}{\sqrt{6}}ix, & x_2 &= -\frac{1}{2}i\beta y, \\ x_3 &= -i\frac{\sqrt{6}}{9}\beta t - i\frac{\sqrt{6}}{9}x, \end{aligned} \tag{40}$$

then the tau function becomes

$$\tau_n = \prod_{i=1}^N (p_i + s_i) e^{\chi_i} \det_{1 \leq i, j \leq N} \overline{m_{i,j}^{(n)}}, \tag{41}$$

where $\overline{m_{i,j}^{(n)}}$ is given by

$$\begin{aligned} \overline{m_{ij}^{(n)}} &= \frac{\tilde{c}_i \delta_{ij}}{(p_i + s_i) e^{\xi_i + \eta_j}} \\ &+ \frac{1}{p_i + q_j} \left(-\frac{p_i}{q_j} \right)^n, \\ \chi_i &= \xi_i + \eta_i = \frac{1}{\sqrt{6}}(p_i + p_i^*)ix - \frac{1}{2}i\beta(p_i^2 - p_i^{*2})y \\ &- \frac{\sqrt{6}}{9}i(p_i^3 + p_i^{*3})(\beta t + x) + \chi_i^0. \end{aligned} \tag{42}$$

When the parameters satisfy $\tilde{c}_{i,j} = 1, s_j = q_j, q_j = p_j^*$, one could conclude that $\chi_i^*(x, y, -t) = \chi_i(x, y, t)$. In this case, we further derive

$$\begin{aligned} \overline{m_{j,i}^{*(-n)}}(x, y, t) &= \overline{m_{i,j}^{(n)}}(-x, y, -t), \\ \tau_n^*(-x, y, -t) &= \tau_n(x, y, t). \end{aligned} \tag{43}$$

Additionally, determining $f = \tau_0, g = \tau_1, h = \tau_{-1}$ and letting

$$p_i = \frac{\omega_i}{2} + i\lambda_i, \quad q_i = \frac{\omega_i}{2} - i\lambda_i, \tag{44}$$

solutions for the breather are discovered.

References

1. Bender, C.M., Boettcher, S.: Real spectra in non-Hermitian Hamiltonians having PT symmetry. *Phys. Rev. Lett.* **80**, 5243–5246 (1998)
2. Yang, J.: General N -solitons and their dynamics in several nonlocal nonlinear Schrödinger equations. *Phys. Rev. E* **383**, 328 (2019)
3. Wen, Z., Yan, Z.: Solitons and their stability in the nonlocal nonlinear Schrödinger equation with PT -symmetric potentials. *Chaos* **27**, 053105 (2017)
4. Hanif, Y., Saleem, U.: Broken and unbroken PT -symmetric solutions of semi-discrete nonlocal nonlinear Schrödinger equation. *Nonlinear Dyn.* **98**, 233–244 (2019)
5. Zhang, Y., Qiu, D., Cheng, Y., He, J.: Rational solution of the nonlocal nonlinear Schrödinger equation and its application in optics. *Rom. J. Phys.* **61**(3), 108 (2017)

6. Ablowitz, M.J., Musslimani, Z.H.: Integrable nonlocal non-linear Schrödinger equation. *Phys. Rev. Lett.* **110**, 064105 (2013)
7. Liu, W., Zheng, X., Li, X.: Bright and dark soliton solutions to the partial reverse space-time nonlocal Mel’nikov equation. *Nonlinear Dyn.* **94**, 2177–2189 (2018)
8. Rao, J., He, J., Mihalache, D., Cheng, Y.: Dynamics of lump-soliton solutions to the PT -symmetric nonlocal Fokas system. *Wave Motion* **101**, 102685 (2021)
9. Fokas, A.S.: Integrable multidimensional versions of the nonlocal nonlinear Schrödinger equation. *Nonlinearity* **29**, 319–324 (2016)
10. Rao, J., Cheng, Y., He, J.: Rational and semirational solutions of the nonlocal Davey–Stewartson equations. *Stud. Appl. Math.* **139**, 568–598 (2017)
11. Yang, B., Chen, Y.: Dynamics of rogue waves in the partially PT -symmetric nonlocal Davey–Stewartson systems. *Commun. Nonlinear Sci. Numer. Simul.* **69**, 287–303 (2019)
12. Liu, Y., Mihalache, D., He, J.: Families of rational solutions of the y -nonlocal Davey–Stewartson II equation. *Nonlinear Dyn.* **90**, 2445 (2017)
13. Matveev, V.B., Salle, M.A.: *Darboux Transformation and Solitons*. Springer, Berlin (1991)
14. Wu, J.: Riemann–Hilbert approach and soliton classification for a nonlocal integrable nonlinear Schrödinger equation of reverse-time type. *Nonlinear Dyn.* **107**, 1127–1139 (2022)
15. Ohta, Y., Yang, J.: Rogue waves in the Davey–Stewartson I equation. *Phys. Rev. E* **86**(3), 036604 (2012)
16. Ohta, Y., Wang, D., Yang, J.: General N -dark-dark solitons in the coupled nonlinear Schrödinger equations. *Stud. Appl. Math.* **127**(4), 345–371 (2011)
17. Ohta, Y., Yang, J.: Dynamics of rogue waves in the Davey–Stewartson II equation. *J. Phys. A: Math. Theor.* **46**(10), 105202 (2013)
18. Yang, X., Zhang, Y., Li, W.: Dynamics of rational and lump-soliton solutions to the reverse space-time nonlocal Hirota–Maccari system. *Rom. J. Phys.* (to appear)
19. Yang, B., Yang, J.: Transformations between nonlocal and local integrable equations. *Stud. Appl. Math.* **140**(2), 178–201 (2018)
20. Maccari, A.: A generalized Hirota equation in $(2+1)$ dimensions. *J. Math. Phys.* **39**, 6547–6551 (1998)
21. Wazwaz, A.M.: Abundant soliton and periodic wave solutions for the coupled Higgs field equation, the Maccari system and the Hirota–Maccari system. *Phys. Scripta* **85**, 065011 (2012)
22. Demiray, S.T., Pandir, Y., Bulut, H.: All exact travelling-wave solutions of Hirota equation and Hirota–Maccari system. *Optik* **127**, 1848–1859 (2016)
23. Shi, C.Y., Fu, H.M., Wu, C.F.: Soliton solutions to the reverse-time nonlocal Davey–Stewartson III equation. *Wave Motion* **104**, 102744 (2021)
24. Yu, X., Gao, Y.T., Sun, Z.Y.: N -soliton solutions for the $(2+1)$ -dimensional Hirota–Maccari equation in fluids, plasmas and optical fibers. *J. Math. Anal. Appl.* **378**, 519–527 (2011)
25. Wang, R., Zhang, Y., Chen, X., et al.: The rational and semirational solutions to the Hirota–Maccari system. *Nonlinear Dyn.* **100**(3), 2767–2778 (2020)
26. Xia, P., Zhang, Y., Zhang, H., et al.: Some novel dynamical behaviours of localized solitary waves for the Hirota–Maccari system. *Nonlinear Dyn.* **108**, 533–541 (2022)

27. Zhou, T., Tian, B., Shen, Y., Gao, X.: Auto-Bäcklund transformations and soliton solutions on the nonzero background for a $(3 + 1)$ -dimensional Korteweg–de Vries–Calogero–Bogoyavlenskii–Schif equation in a fluid. *Nonlinear Dyn.* **111**, 8647–8658 (2023)
28. Rao, J., He, J., Mihalache, D., Cheng, Y.: PT -symmetric nonlocal Dave–Stewartson I equation: general lump-soliton solutions on a background of periodic line waves. *Appl. Math. Lett.* **104**, 106246 (2020)
29. Jiang, D., Zha, Q.: Breathers and higher order rogue waves on the double-periodic background for the nonlocal Gerdjikov–Ivanov equation. *Nonlinear Dyn.* **111**, 10459–10472 (2023)
30. Liu, Y., Li, B.: Dynamics of solitons and breathers on a periodic waves background in the nonlocal Mel’nikov equation. *Nonlinear Dyn.* **100**, 3717–3731 (2020)
31. Hirota, R.: *The Direct Method in Soliton Theory*. Cambridge University Press, Cambridge (2004)
32. Sato, M.: Soliton equations as dynamical systems on infinite dimensional Grassmann manifold. *North-Holland Math. Stud.* **81**, 259–271 (1983)

Publisher’s Note Springer Nature remains neutral with regard to jurisdictional claims in published maps and institutional affiliations.

Springer Nature or its licensor (e.g. a society or other partner) holds exclusive rights to this article under a publishing agreement with the author(s) or other rightsholder(s); author self-archiving of the accepted manuscript version of this article is solely governed by the terms of such publishing agreement and applicable law.